Improving Power System Reliability through Optimization via Simulation

Rafael Sacaan
Hugh Rudnick
Department of Electrical Engineering
Pontificia Universidad Católica
Santiago, Chile

Tomás Lagos
Fernando Ordóñez
Department of Industrial Engineering
Universidad de Chile
Santiago, Chile

Alejandro Navarro-Espinosa
Rodrigo Moreno*
Department of Electrical Engineering
Universidad de Chile/Imperial College*
Santiago, Chile/London, UK

***Abstract*—Due to the stochastic nature of equipment failures, the accurate assessment of power system reliability is a complex task. Consequently, the optimal selection of new network infrastructure to improve reliability is even harder. In this paper, an optimization via simulation approach is proposed to find the optimal set of network assets to improve system reliability. Particularly, an Industrial Strength COMPASS algorithm is implemented to find the optimal set of new transmission lines that maximizes system reliability subject to a budget constraint. This algorithm iteratively proposes, in a first stage, a set of new transmission lines that are then tested, in a second stage, via simulation of the system operation, including impact of various network failures. In the second stage, the sequence day-ahead unit commitment plus real-time operation is modeled along with a sequential Monte Carlo simulation to determine highly detailed system operation under network outages and thus calculate the associated expected energy not supplied.**

***Index Terms* — Reliability Analysis, Sequential Monte Carlo Simulations, Optimization via Simulations.**

I. INTRODUCTION

Reliability has been historically a crucial topic in power systems [1], remaining very relevant until today. In fact, many countries are incorporating tighter limits to their reliability indices in order to reach higher security levels, even under the occurrence of natural hazards [2]. These reliability improvements, however, drive additional costs and thus need to be efficiently determined to ensure an adequate benefit/cost ratio. Hence the optimal level of reliability can be found by balancing the reliability benefits (generally measured as savings in expected cost of unsupplied demand) against the required cost of operation and/or investment to improve reliability [3].

It is important to highlight that the reliability can be increased by both investment in conventional assets (e.g., transmission lines, power plants, etc.) and by operational measures (that may also drive smaller volumes of investment in ICT infrastructure) such as demand side response [4], [5]. For instance, reference [5] develops a framework to deliver various levels of reliability for different consumers by using load control. These approaches can support improvements in reliability, defer new investment and even, in some cases, eliminate the need for additional infrastructure [6].

The reliability impact of a particular network investment (i.e., a new line or transformer) can be determined by both analytical and simulation techniques [7]. The former uses mathematical models to find exact mathematical solutions (and includes often important simplifications). The latter instead uses Monte Carlo simulations to represent the stochastic nature of contingencies in power systems [7]. These simulations can be (i) non-sequential, meaning that the time intervals are assumed independent, or (ii) sequential, where the chronological time dependence is considered [8]. This characteristic is paramount to incorporate the effects of load variations across a day and to properly include the recovery times of different facilities after a failure occurs. By using this approach, failure rates and the corresponding recovery times can be incorporated for each system asset, and therefore adequate quantification of system reliability can be undertaken through simulation of possible combinations of faults (sampling can also be used to reduce number of events). Hence, reliability analysis of a new transmission line requires a complete set of simulations with and without the new asset to quantify its reliability benefits. Likewise, reliability analysis of a portfolio of candidate transmission lines requires a very large number of simulations that may be intractable.

In this vein, the main contribution of this paper is to propose an optimization via simulation (OvS) approach to determine new network investment based on reliability improvements. In particular, we illustrate, for the first time, the use of the Industrial Strength COMPASS algorithm [9] to find an optimal portfolio of new network assets that improves system reliability whilst considering (i) detailed representation of power system operation (including simulation of both day-ahead unit commitment and real-time operation) and (ii) detailed simulation of faults (including chronological dependence between failures, components and recovery times modelled through sequential Monte Carlo simulations (SMCs)). Specifically, OvS finds the best solution in a optimization problem based on the expected performance (e.g., expected energy not supplied, hereinafter EENS) of a system under the realizations of multiple scenarios/faults (power systems with SMCs) [10].

The rest of the paper is structured as follows. Section II describes the proposed methodology. The interactions between the power system simulation and the optimization problem are presented through two case studies in section III. Finally, the main conclusions are drawn in section IV.

II. METHODOLOGY

In this section, the two main parts of the proposed methodology are presented. Firstly, the operation and SMCs models are shown, followed by the OvS approach.

A. Detailed operation and fault representation: Day-ahead unit commitment, real-time operation and sequential Monte Carlo analysis

In order to carry out an accurate reliability analysis within a given horizon (e.g., a day), it is important to represent network operation in detail. To do so, we first determine the schedule operation through a unit commitment problem and then (when on/off status of each generating unit is fixed) we simulate real time operation through a DC-OPF problem. While the unit commitment problem is run on an intact system scenario (no faults), real time operation is subject to fault occurrence. Hence the expected unsupplied energy will depend on both system infrastructure and operational features such as the amount of reserve scheduled, the ramp rate limits of generating units, startup times, etc. The abovementioned model has the following three main modules.

1) Unit commitment: An hourly generation scheduling plan is determined over a 24-hour horizon, where the overall operation cost is minimized. An extension of the mixed-integer linear programming formulation presented in [11] has been developed to consider a multi-busbar network with capacity constraints. Each unit is modelled by using variable costs, startup costs, shutdown cost, minimum stable generation, maximum power output, ramp rate constraints (up and down), minimum downtime and minimum uptime. Furthermore, a spinning reserve requirement for each hour has been included.

2) DC-OPF: Given the on/off status of generating units (determined by the unit commitment problem) a DC optimal power flow is applied to determine the real time operation of the power system when this is re-dispatched after a fault occurs. Hence, this linear programing problem (DC-OPF) determines the production for every unit at each period/hour in order to meet supply and demand at minimum cost. The cost function is to minimize total production cost including the cost of energy not supplied (ENS) at each busbar. Thus, if an outage occurs, the DC-OPF will provide a solution that minimizes the aforementioned cost function. Finally, the DC-OPF outputs the optimal production from each unit and the ENS at each busbar.

3) Sequential Monte Carlo: This refers to the generation of stochastic scenarios through Sequential Monte Carlo Simulation (SMC), modelling network failures. We consider that each transmission line features a constant failure rate λ (occurrences per hour), and a constant recovery time *r* (hours). The model considers a large number of failure combinations across a day and also considers equipment out of services because of faults during previous hours. Similarly, the model puts equipment back in service when recovery time has expired.

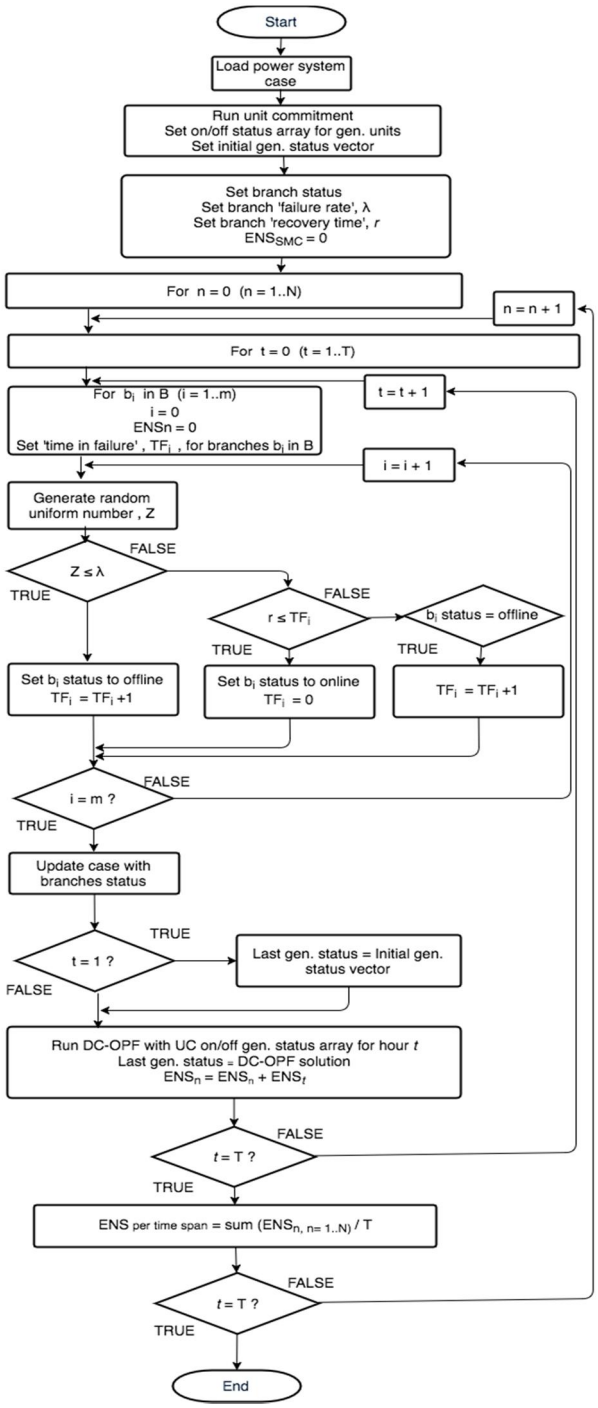

Figure 1. SMCs Flowchart.

The complete algorithm to determine system operation under several faults and calculate reliability is presented in Fig. 1, showing the interactions among the unit commitment, DC-OPF and SMC modules. Specifically, this figure shows that at the beginning of the process a day-ahead unit commitment is calculated once. Then, SMCs are executed N times (i.e., simulations). Each simulation starts at hour t (with t = 1...T) and, in each t, it iterates over the set of transmission lines/branches B, where b_i represents branch i (with i = 1...m). For b_i, a uniform random number Z is generated. If Z is less than the failure rate λ, b_i fails. In this case, parameters TF_i

(failure duration time of branch i) and b_i status are updated. If the recovery time r is less than TF_i, the branch is brought online. Finally, if branch i was already offline, parameter TF_i is updated. Given the new online/offline status for the set of branches in hour t, a DC-OPF is executed for this hour, considering as an initial condition the production of generating units calculated by the DC-OPF in hour t-1. The output of the DC-OPF module corresponds to generation production and the ENS in hour t. This process is repeated until t reaches T (24 hours), completing one simulation. The whole SMC is completed when N simulations of a day have been executed. Each system's branch status is set to a default value whenever a simulation starts over again. The final output is the EENS in the entire simulation horizon (e.g., 24 hours).

B. Optimization via Simulation

Optimization via simulation (OvS) refers to finding the best solution (maximization or minimization) according to the expected performance (i.e. average index) of a system under the realizations of multiple scenarios. OvS algorithms explore more promising solution regions while utilizing some form of randomization to escape local optimal regions; this last feature allows these algorithms to visit all solutions at least once if the algorithm is executed for infinite time [10]. In this work, since a feasible region is integer valued, a Discrete OvS (DOvS) is used. This problem can be formulated as follows:

$$\min_{x\in\Theta}\{g(x) = E_x[Y(x)]\} \qquad \Theta = \Phi \cap Z^d, \tag{1}$$

where $\Phi \subset R^d$ is a set that could be bounded or unbounded. There are some DOvS algorithms developed in the literature, such as the stochastic ruler method [12], variants of simulated annealing changed to accommodate randomness [13], the COMPASS (Convergent Optimization via Most Promising Area Stochastic Search) algorithm [14], and the Industrial Strength COMPASS (ISC) [9]. The ISC comprises three stages: (i) noise sampling scheme, (ii) finding local optimal regions (also called niches), and (ii) comparing various local optimum solutions in a Ranking and Selection (R&S) framework [9].

Furthermore, this approach makes no assumption on the structure of the objective function and thus allows to model large and complex problems. Hence, the problem of finding the optimal set of new network components to increase reliability considering a detailed power system modelling and its chronological dependence of failures and recovery times (Section II.A), is solved by using DOvS and specifically ISC.

In this procedure, the output $F(x, \xi)$ of a single simulation is considered to come from a "black box" model, whose internal structure remains unknown to the solving scheme. One specific system simulation, x (where x is a binary vector that represents if a set of lines is either built or not), will return the energy not supplied $F(\cdot)$ for a scenario realization ξ (i.e., daily simulation with a potential realization of multiple failures). The objective is to minimize the expected energy not supplied subject to a resource budget constraint as shown in (2):

$$min_{x\in\,\Theta}\{G(x) = E_\xi[F(x,\xi)]\} \tag{2}$$

$$\Theta = \{x: \sum_{i=1}^{d} a_{ij}\, x_i \le b_j, \quad j = 1,\dots,p \tag{3}$$

$$0 \le x_i \le 1, \quad i = 1,\dots,d \tag{4}$$

$$x_i \in Z^d, \quad i = 1,\dots,d \tag{5}$$

The next subsections explain each of the ISC stages.

1) Niching Genetic Algorithms (NGA): The role of the NGA is to serve as a global search engine. It forms niches (Fig. 2) that have always at the center a local optimal solution. Transition rules to the local convergence are:

- Niche rule: If at any time, there is only one niche.
- Budget rule: If the number of samples is exceeded.
- Improvement rule: If there are no better solutions in a number of consequent iterations.
- Dominance rule: If the solutions within one niche dominate all other niches. Let I be the set that contains niches that are statistically better than others in terms of average quality of individuals within those niches. If $|I| = 1$, then there is a dominant niche and NGA stops.

Fitness sharing scheme is implemented in the algorithm. The idea is that if a niche is populated with too many solutions, these solutions should be given less chance to reproduce than they would have had in an ordinary GA, thus allowing solutions in less populated niches to have higher probabilities of being selected to generate new solutions. Grouping procedure is done to form groups that are similar in their fitness value. For each of these, an average probability of selection $m_j^i = \frac{1}{N_i}\left(\sum_{j=1}^{N_i} s_j^i\right)$ is calculated, where s_j^i is the probability of selecting an individual j within the population defined by $[N_i]$; this probability is calculated as $s_i = \frac{1}{m_G}(\eta - 2(\eta-1)\left(\frac{i-1}{m_G-1}\right))$. Then, the Stochastic Universal Sampling (SUS) section considers a roulette wheel (i.e., circle area divided in slices), where the area for each individual is proportional to its selection probability. The roulette wheel is spun once (i.e., a uniform number between 0 and 1 selects the position of a pointer in the circle) and an individual is selected as a parent. Other individuals can be selected by moving the pointer forward several times when considering a regular spacing of $\frac{2}{m_G}$until it goes back to the starting point.

The additional stages of the NGA are similar to the classical approach taken in GA literature and it includes a Mating Restriction scheme to select partners after SUS, then a Crossover scheme is applied to combine the parents' genes, and a Mutation scheme to determine new solutions.

*2) COMPASS:*This step refers to the convergence to a local optimum point in each niche. So this procedure starts with a population of individuals within a niche. Denote the set V_k as all solutions visited at iteration k. Let $C_k = \{x \in \Theta \,|\, ||x - \hat{x}_k|| \le ||x - y||, \forall y \in V_k, y \ne \hat{x}_k\}$ be the most promising area at iteration k.

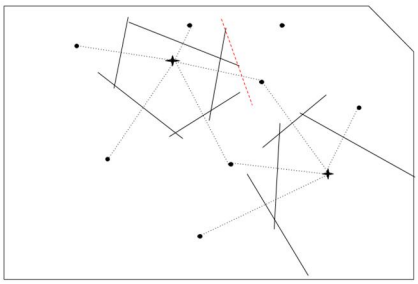

Figure 2. Most promising area around two niches.

Require: Set $k = 0$, find $x_0 \in \Theta$, set $V_0 = \{x_0\}$. Determine $a_0(x_0)$, and take $a_0(x_0)$ observations from $g(x_0)$. Calculate $\bar{G}_0(x_0)$ and $N_0(x_0) = a_0(x_0)$.

1- Let $k = k + 1$. Sample $x_{k1}, \ldots, x_{km} \in C_{k-1}$ uniformly and independently. Let $V_k = V_{k-1} \cup \{x_{k1}, \ldots, x_{km}\}$. For every $x \in V_k$ take $a_k(x)$ observations and update $N_k(x)$ and $\bar{G}_k(x)$.

2.- Let $\hat{x}_k^* = \text{argmin}_{x \in V_k}\{\bar{G}_k(x)\}$, and construct C_k.

3.- Go to line 1

Figure 3. Main loop of the local convergence stage.

For instance, in Fig. 2 the crosses have a better performance measure than all the neighbors that define active constraints, the point with the best performance measure in the niche is referred as the head of the niche. This figure shows that the upper right point is within a non-niched structure since at least one of its three neighbors presents a better performance, and it do not define any active binding constraint in any head of niche.

Fig. 3 displays the COMPASS algorithm. There, the function $a_k(x)$ represents the sampling allocation rule (SAR) that assigns the number of evaluations to each solution at iteration k. The COMPASS algorithm converges to a local optimal solution as $k \to \infty$, under very mild conditions, meaning that each sample's expected value satisfies a strong law of large numbers, and the SAR guarantees that the number of replications allocated to all visited solutions goes to infinity. Let $N(x) = \{y \in \Theta | \, ||x - y|| \leq 1\}$. Given a local solution $\hat{x}_k^*$ of a specific niche, the Transition Rule follows the hypothesis test:

$$\begin{aligned} H_0 &: G(\hat{x}_k^*) \leq \min_{y \in N(\hat{x}_k^*)} G(y) \\ H_1 &: G(\hat{x}_k^*) > \min_{y \in N(\hat{x}_k^*)} G(y) \end{aligned} \tag{6}$$

The type I error is set to α_L and the power of the test to be at least $1 - \alpha_L$ if $g(\hat{x}_k^*) \leq \min_{y \in N(\hat{x}_k^*)} g(y) + \delta_L$, where δ_L is a tolerance value (specified by the user). The test can be re-written as:

$$\begin{aligned} &\Pr\{declare\ \hat{x}^*\ locally\ optimal\} \geq 1 - \alpha_L, \\ &\quad if\ \bar{G}(\hat{x}^*) \leq \min_{y \in N(\hat{x}^*)} \bar{G}(y) \\ &\Pr\{declare\ \hat{x}^*\ not\ locally\ optimal\} \geq 1 - \alpha_L, \\ &\quad if\ \bar{G}(\hat{x}^*) \geq \min_{y \in N(\hat{x}^*)} \bar{G}(y) + \delta_L \end{aligned} \tag{7}$$

If the solution past the test, the current COMPASS iteration over the niche is stopped and $\hat{x}_k^*$ is declared as local optimal.

3) Clean-up phase: Once the COMPASS local search has exhausted all niches found by the NGA global search, or the budget has run out, ISC enters the clean-up phase. The objective of this step is to compare the found local optimal solutions to select the best of them, or one within δ_G of the best, with high confidence, stating a $\pm\delta_G$ confidence interval on the performance of the selected solution. The user can specify parameters δ_G and α_G. The stages on this phase are as follows [15]:

- Screening: Using the data already available about the solutions in L (which is the set of indexes of locals optimal obtained in the local stage phase), it discards any solutions that can be proved to be statistically poorer than others. Let L_C be the surviving solutions.
- Selection: Acquire enough additional replications on the solutions in L_C to select the best. Let x_B be the selected solution.
- Estimation: With confidence level $\leq 1 - \alpha_G$, x_B is the best, or within δ_G of the bests.

The solution determined by the ISC algorithm corresponds to the set of new network infrastructure that are optimal and thus minimize the expected energy not supplied, EENS.

III. Case Study

A. IEEE 14-busbar test system

1) Sytem operation under fault conditions

The IEEE 14-busbar test system is used, which has 5 generators, 19 transmission lines/transformer and 11 loads (Fig. 4). The system was modified in order to satisfy simulation requirements by 1) adding more technical/economic parameters to generating units (such as minimum power outputs, ramp rate limits, minimum downtimes and uptimes, and the costs of production, startup and shutdown), 2) adding transmission features (active power capacity) and 3) considering a load profile. The main system's characteristics are presented in the Appendix.

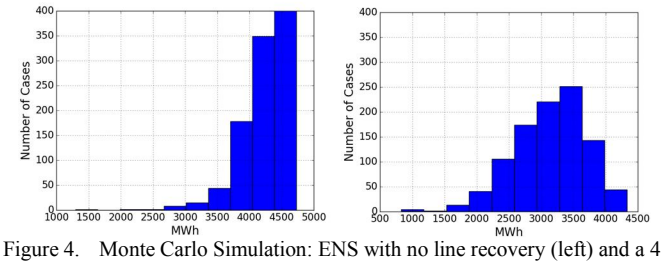

Figure 4. Monte Carlo Simulation: ENS with no line recovery (left) and a 4 hour recovery time (right).

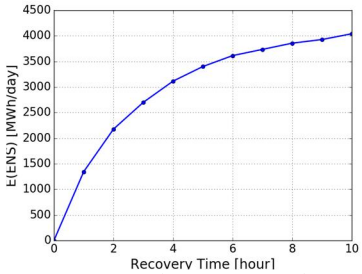

Figure 5. Recovery time vs. Expected ENS per day.

The Monte Carlo simulation method has four parameters: network/line failure rates λ (occurrences per hour), recovery time r (hours), number of Monte Carlo runs N=1000, and time horizon of each run T= 24 hours. As an application example, if the failure rate is set to 0.05 for each line with no line recovery (i.e. line is maintained outaged during the remaining simulation horizon after a fault occurs), the expected ENS is 4234.32 MWh/day. Now, if recovery time is set to 4 hours for every line, the expected ENS is 3143.59 MWh/day. The corresponding histograms are presented for both simulations in Fig. 5.

Recovery times affect system reliability and therefore they must be modelled adequately. In fact, as recovery times increase, the expected energy not supplied (EENS) escalates considerably. In Fig. 6, the EENS for different recovery times is plotted. A recovery time equal to zero means that once a line has failed, it is brought online immediately.

2) Sytem investment to improve reliability

We use the previous reliability assessment process that determines the energy not supplied in scenario realization ξ, to run the ISC algorithm and determine the optimal network investment. A binary vector $x \in \{0,1\}^{|A|}$ represents the decision of installing candidate lines, where $A = \{(i,j) \in V \times V \setminus E\}$, V is the set of existing buses and E is the set of existing lines or branches. We consider a budget of 1 and 3 new lines (i.e. $b = 1$ and $b = 3$).

The case study is solved by using two methods: (i) that proposed in this paper and (ii) full-enumeration. For $b = 1$ the number of possible integer solutions is $1 + 71, |A| = 72$, (71 feasible lines plus the possibility of 0 lines), in this case a full enumeration approach (that assesses all feasible solutions) is able to find the optimal solution in approximately 143 minutes (2000 evaluations to each solution).

Table I and II show the results for the case study assuming a recovery time of 2 hours. Notice that in these tables, the field Evaluations (Eval.) refers to the number of simulations performed in each stage of the solution process (in this case, the ISC run significantly less evaluations than the full-enumeration approach). The best solution obtained through the ISC needed 1581 evaluations to pass the tests (Table I). It is important to highlight that the proposed methodology needs less evaluations since it is not further exploring poor solutions.

In addition, this methodology was run with a budget of 3 lines, where the number of possible solutions is equal to $1 + 71 + 71 \cdot 70 + 71 \cdot 70 \cdot 69 = 347{,}972$ (all possible combinations of 0, 1, 2 and 3 lines). The results are summarized in Table III and IV, where Table III comprises three potential solutions since, statistically speaking, the best solution cannot be recognized ($1 - \alpha_G = 90\%$ confidence is binding). Finally, Table IV indicates that the simulation time to determine the best solution when the budget is equal to 3 (among the 347,972 feasible combinations) was 141 minutes.

TABLE I. ISC RESULTS 14 BUSBARS – BUDGET OF 1 LINE (NEW LINES ARE IDENTIFIED THROUGH ITS FROM AND TO NODES AS FOLLOWS: [FROM,TO]).

New line	EENS [MWh]	Eval. [#]	Coeff. of Var.
[1,9]	1751.88	1518	0.234

TABLE II. PERFORMANCE RESULTS 14 BUSBARS – BUDGET OF 1 LINE

Algorithm	Time [min]	Eval. [#]	Stage	NGA	COM	R&S
Full Enu.	143	144000	Time [min]	0.7	4	7.2
ISC	12	11388	Eval. [#]	480	3687	7221

TABLE III. ISC RESULTS 14 BUSBARS – BUDGET OF 3 LINES

New lines	EENS [MWh]	Eval. [#]	Coeff. of Var.
[1,3] [1,9]	1553.72	1765	0.242
[1,3] [1,9] [6,10]	1555.71	1325	0.25
[1,3] [1,9] [11,14]	1574.44	898	0.248

TABLE IV. PERFORMANCE RESULTS 14 BUSBARS – BUDGET OF 3 LINES

Stage	NGA	COM	R&S	Total
Time [min]	2.42	137	2.3	141.7
Eval. [#]	1440	112667	2117	116224

B. IEEE 57-busbar test system

1) Sytem operation and investment

With the purpose of testing the scalability of the proposed methodology, a larger analysis was carried out for the IEEE 57-busbar test system. The same set of parameters from the 14-busbar case was considered here.

When the recovery time is set to 3 hours, the expected energy not supplied is equal to 2389.5 MWh/day. When we consider that the outaged line is not restored after a fault occurs, the EENS increases to 5151.08MWh/day. As in the previous case, we determine solutions for a budget of 1 and 3 new lines. Note that, in this case, the problem has approximately 3.5 million of possible solutions (for b=3). The parameters of tolerance and statistical significance were maintained as in the previous case. Tables V to VIII summary the main results.

TABLE V. ISC RESULTS 57 BUSBARS– BUDGET OF 1 LINE

New lines	EENS [MWh]	Eval. [#]	Coeff. of Var.
[2, 24]	2361.62	457	0.133
[31, 40]	2392.83	662	0.132

TABLE VI. PERFORMANCE RESULTS 57 BUSBARS– BUDGET OF 1 LINE

Stage	NGA	COM	R&S	Total
Time [min]	290.37	38.71	4.19	350.85
Eval. [#]	6700	6446	1095	14241

TABLE VII. ISC RESULTS 57 BUSBARS– BUDGET OF 3 LINES

New lines	EENS [MWh]	Eval. [#]	Coeff. of Var.
[3, 49], [6, 44], [9, 47]	2080.77	607	0.163

TABLE VIII. PERFORMANCE RESULTS 57 BUSBARS– BUDGET OF 3 LINES

Stage	NGA	COM	R&S	Total
Time [min]	405.30	168.84	5.12	579.26
Eval. [#]	14210	8393	1306	23909

For b=1, the solutions present less evaluations than in the14-busbar case (comparison between Tables I and V); this is because of the performance of the solutions that were compared during the optimization process. Two measures affect the quality of the convergence, the variance and the performance level among the solutions. Both of these measures are greater in the 14-busbar case than in the 57-busbar case. It is worth noticing that in Table I, the coefficient of variance is larger than in Table V. In fact, a lower coefficient of variance produces more accurate estimates with fewer evaluations. The same characteristic can be observed when b=3, where the coefficients of variance in Table III (14-busbar) are larger than those in Table VII.

Furthermore, it is not possible to directly compare the number of evaluations used in each case study, since the searching space is bigger in the 57-busbar. Although the effort spent in the 14-busbar network is greater (i.e., number of evaluations per solution candidate for both budgets, b=1 and b=3), the complete process takes longer in the 57-busbar example because of the increased number of variables. This can be observed by comparing the simulation time and number of evaluations between Tables II and VI for b=1, and Tables IV and VIII for b=3.

It is important to highlight that Table III (14-busbar and b=3) and Table V (57 bus-bar and b=1) present more than one optimal solution because these solutions cannot be, statistically speaking, differentiated due to their poor statistical significance. On the contrary, Tables I (14-busbar and b=1) and VII (57 bus-bar and b=3) show only one optimal solution for each case because after the COMPASS stage is executed, it was possible to find one unique solution by using the R&S procedure.

IV. CONCLUSIONS

We propose an optimization via simulation approach to identify optimal portfolios of network investment that improve system reliability. The model considers a highly detailed representation of system operation while considering the occurrence of an array of network failures (i.e. three-fold unit commitment, DC-OPF and sequential Monte Carlo modeling). The proposed optimization via simulation approach allows both efficient calculation of the solution and a highly detailed modelling of system operation, including impact of outages on unsupplied demand across time (i.e. recovery). The proposed approach was applied on the IEEE 14-bus and 57-bus systems, demonstrating its ability to find good solutions in reasonable timescales.

APPENDIX

Generation plants data from the IEEE 14-busbar case (5 generation units and 19 lines) and the IEEE 57-busbar case (7 generation units and 80 lines) can be found in [16]. Capacities of new lines have been set equal to 100 MW in the 14-busbar case and 200MW in the 57-busbar network, respectively. For both cases, the reactance of new lines is 0.05 p.u. and the value of lost load is assumed to be 10,000 $/MWh on each busbar.

ACKNOWLEDGMENT

The authors gratefully acknowledge the financial support of UK Research Council and Conicyt through the grant Newton-Picarte (MR/N026721/1).

REFERENCES

[1] R. Allan, “Power system reliability assessment-A conceptual and historical review,” *Reliab. Eng. Syst. Saf.*, vol. 46, no. 1, pp. 3–13, 1994.

[2] M. Panteli and P. Mancarella, “Modeling and Evaluating the Resilience of Critical Electrical Power Infrastructure to Extreme Weather Events,” *IEEE Syst. Journal,* pp. 1–10, 2015.

[3] R. N. Allan and R. Billinton, “Probabilistic methods applied to electric power systems - are they worth it?,” *Power Eng. J.*, pp. 121–129, 1992.

[4] D. Huang and R. Billinton, “Impacts of demand side management on bulk system reliability evaluation considering load forecast uncertainty,” *2011 IEEE Electr. Power Energy Conf. EPEC 2011*, no. 2, pp. 272–277, 2011.

[5] A. L. A. Syrri and P. Mancarella, “Reliability and risk assessment of post-contingency demand response in smart distribution networks,” *Sustain. Energy, Grids Networks*, vol. 7, pp. 1–12, 2016.

[6] R. Moreno, D. Pudjianto, and G. Strbac, “Security and Corrective Control,” *IEEE Trans. Power Syst.*, vol. 28, no. 4, pp. 3935–3944, 2013.

[7] R. Allan and R. Billinton, “Probabilistic assessment of power systems,” *Proc. IEEE*, vol. 88, no. 2, pp. 140–162, 2000.

[8] R. Billinton, H. Chen, and R. Ghajar, “Time-series models for reliability evaluation of power systems including wind energy,” *Microelectron. Reliab.*, vol. 36, no. 9, pp. 1253–1261, 1996.

[9] J. Xu, B. L. Nelson, and L. J. Hong, “Industrial strength COMPASS,” *ACM Trans. Model. Comput. Simul.*, vol. 20, no. 1, pp. 1–29, 2010.

[10] L. Hong and B. Nelson, “A brief introduction to optimization via simulation,” *Winter Simul. Conf.*, no. 2002, pp. 75–85, 2009.

[11] M. Carrión and J. M. Arroyo, “A computationally efficient mixed-integer linear formulation for the thermal unit commitment problem,” *IEEE Trans. Power Syst.*, vol. 21, no. 3, pp. 1371–1378, 2006.

[12] D. Yan and H. Mukai, “Stochastic Discrete Optimization,” *SIAM J. Control Optim.*, vol. 30, no. 3, pp. 594–612, 1992.

[13] M. H. Alrefaei and S. Andradóttir, “A Simulated Annealing Algorithm with Constant Temperature for Discrete . Stochastic Optimization,” *Management*, no. 5, 1999.

[14] L. J. Hong and B. L. Nelson, “Discrete Optimization via Simulation Using COMPASS,” *Oper. Res.*, vol. 54, no. 1, pp. 115–129, 2006.

[15] J. Boesel, B. L. Nelson, and S.-H. Kim, “Using Ranking and Selection to ‘Clean Up’ after Simulation Optimization,” *Oper. Res.*, vol. 51, no. 5, pp. 814–825, 2003.

[16] IEEE test systems. Available at (accessed March 12, 2017): www2.ee.washington.edu/research/pstca/pf14/pg_tca14bus.htm & www2.ee.washington.edu/research/pstca/pf57/pg_tca57bus.htm